

Supplemental Information

Local inflammation but not kidney cell infection associated with high *APOL1* expression in COVID-associated nephropathy

Methods

APOL1 genotyping

Infiltrate scoring

Immunofluorescence

In situ hybridization

Quantification with QuPath

Reagent List

Tables

Supplemental Table 1. Details on subjects in biopsy cohort.

Figures

Supplemental Figure 1. Assay and tissue validation with control probes and control tissues.

Supplemental Figure 2. Common artifacts (false positives) of the ACDBio RNAscope in situ hybridization method using chromogenic stains.

Supplemental Figure 3. Immune cells in autopsy and biopsy kidney tissue.

Supplemental References

Methods

APOL1 genotyping

Genomic DNA extractions were from formalin-fixed, paraffin-embedded kidney sections scraped from glass slides (1-2 sections per extraction, depended on amount of tissue on slide). DNA was extracted using the Qiagen RecoverAll total nucleic acid isolation kit following recommended deparaffinization procedures. Final DNA elution was with DNA/RNA-free, DNase/RNase-free water. DNA concentrations were estimated by optical density using spot samples and 5-10ng of DNA were used per each assay. Genotyping for *APOL1* polymorphisms used the TaqMan allele discrimination assay (Thermo Fisher Scientific) for the G1 allele (rs73885319, assay ID C98253221) and G2 allele (rs71785313, assay ID C102754756). Using the dry down method, DNA was pipetted into 384 reaction plates and air dried overnight. TaqPath ProAmp Master Mix (Thermo Fisher Scientific) was mixed with the appropriate TaqMan assay mix for a final volume of 5µl, which was pipetted into each well (positive and negative controls were included on each plate). Amplification used the QuantStudio5 thermocycler (Applied Biosystems) running the QuantStudio Template and Analysis software and using the pre-programmed genotyping amplification protocol (hot start, followed by 40 cycles of 95°C melt for 15 seconds, 60°C amplification for 1 min).

Infiltrate scoring

Renal biopsies were performed for clinically indicated reasons (proteinuria, acute kidney injury) and pathological evaluations were performed by two renal pathologists using standard definitions. Tubulointerstitial lymphocytic inflammation was scored from H&E or PAS stained sections using a semiquantitative scale (0; negative or trace/rare presence of inflammatory cells; 1+, <20% of the tubulointerstitium affected; 2+, 20-40% of the tubulointerstitium affected; 3+, 41-60% of the tubulointerstitium affected; 4+, >60% of the tubulointerstitium affected). All available tissue was scored, which was primarily cortex, but some sections contained medullary tissue.

Immunofluorescence Microscopy

Protein detection by antibody mediated immunofluorescence microscopy with antigen retrieval has been previously described.¹ Sources and specifications of antibodies used are provided in the attached Reagent List. APOL1 antibody specificity has been examined and validated previously.² Formalin-fixed, paraffin-embedded 4µm sections were mounted on Fisher superfrost glass slides and were cleared with xylenes, rehydrated in ethanol and washed in water. Antigen retrieval was in 10 mM trisodium citrate dihydrate 6.0, 0.05% Tween-20 using a pressure cooker,

boiling under pressure for 4.5 min. Slides were cooled to room temperature, rinsed in PBS, and transferred to PBST (PBS with 0.2% Tween-20). Slides were blocked with 5% normal goat serum in PBST for 1 hour, and incubated overnight at 4°C in PBS, 1% normal goat serum, 0.1% Tween-20 with the appropriate dilution of primary antibodies (see Reagent Table). Following incubation, slides were washed with PBST, and incubated with species specific fluorophore-conjugated secondary antibody in PBS for 1 hour at room temperature and washed with PBST. Slides were mounted in antifade mounting media containing DAPI. Fluorescent images (2048 x 2048 pixels, 72 pixels/inch) were captured using Leica LAS-X software on a Leica TS-SP8-AOBS inverted confocal microscope using 405, 488, and 561 lasers at 40X magnification.

In situ hybridization

The RNA in situ hybridization for gene expression was performed using manual kits from ACDBio following kit instructions (See Reagent List for details on kits and probes). Manual tissue pretreatment conditions (target retrieval and protease digestion) for both lung and kidney tissue were 15 minute boiling and 30 minute protease digestion. Samples that failed under these conditions were repeated with modifications to the pretreatments (combinations of boiling times ranging from 10 to 30 minutes, and protease digestion times ranging from 10 to 30 minutes). However, failed samples continued to fail under these optimizing runs and likely represented samples with significant RNA degradation. Other than optimizing tissue pretreatment conditions, there was no deviation from the provided kit protocol. Slides were mounted in EcoMount, dried overnight, and visualized using light microscopy (see below).

The fluorescent in situ hybridization (FISH) procedure to detect bacteria used 5'-labeled Alexa fluor 660 DNA probes (synthesized at Invitrogen) and conditions as previously described.³ Briefly, deparaffinized tissue sections were incubated with the FISH probe (3ng/μl, see Reagent List) in hybridization buffer (100 mM Tris-HCl pH 7.2, 0.9 M NaCl, and 0.1% SDS, and RNA stabilization solution) using 50 μl/slide, and a cover slip was floated on the tissue section, followed by incubation for 90 minutes at 60°C. Coverslips were removed and slides were washed with 100 mM of Tris-HCL pH 7.2, 0.9 M NaCl, 0.1 mM SDS for 30 minutes. Slides were mounted in antifade mounting media with DAPI and imaged as described above for immunofluorescence microscopy.

Quantification of gene expression.

ACDBio recommends QuPath,⁴ an open source (<https://qupath.github.io/>) digital pathology and image analysis program, for quantification of single molecule detections. QuPath file and stain definitions were programmed as recommended by ACDBio in their analysis guidelines (<https://acdbio.com/qupath-rna-ish-analysis>) and parameters used in cell and spot detection are summarized in the adjacent table. Of note, in high expressing cells any signal clusters (i.e., the merging or overlap of single molecule signals) were quantified using the "split by intensity" method. Light micrograph images (TIFF format, 1024 x 1280 pixels, 72 pixels/inch) at 40X magnification were collected on a Nikon Eclipse 55i microscope using Nikon Digital Sight 10 frame capture and NIS Elements software (Nikon). Raw images were imported into QuPath and manually annotated for individual glomeruli (all available in biopsies) or proximal tubules (an average of eight tubules per specimen from three separate 40X fields). Biopsy cores that had less than three glomeruli were excluded from single cell quantifications. Data output for subcellular detections was collected for both the annotated region (used for whole glomeruli scoring) and for each cell within the annotated region (used for single cell scoring). QuPath also provided data for areas and volumes for both annotated regions and cells, with volumes calculated based on a specimen thickness of 4µm.

QuPath settings		Glomeruli	Proximal tubule	
nucleus parameters	background radius	40	40	
	median fl radius	0	0	
	sigma	6	8	
	min area	150	450	
	max area	1500	2000	
	threshold	0.1 to 1.5	0.05 to 0.1	
	max background	2	2	
	split by shape	yes	yes	
	cell parameters	cell expansion	75	30
		include nucleus	yes	yes
smooth boundaries		yes	yes	
subcellular spot detection	detect threshold	0.2	0.2	
	smooth	no	no	
	split by shape	no	no	
	split by intensity	yes	yes	
spot & cluster parameters	expect spot size	1	1	
	min spot size	1	1	
	max spot size	200	50	
	include clusters	yes	yes	

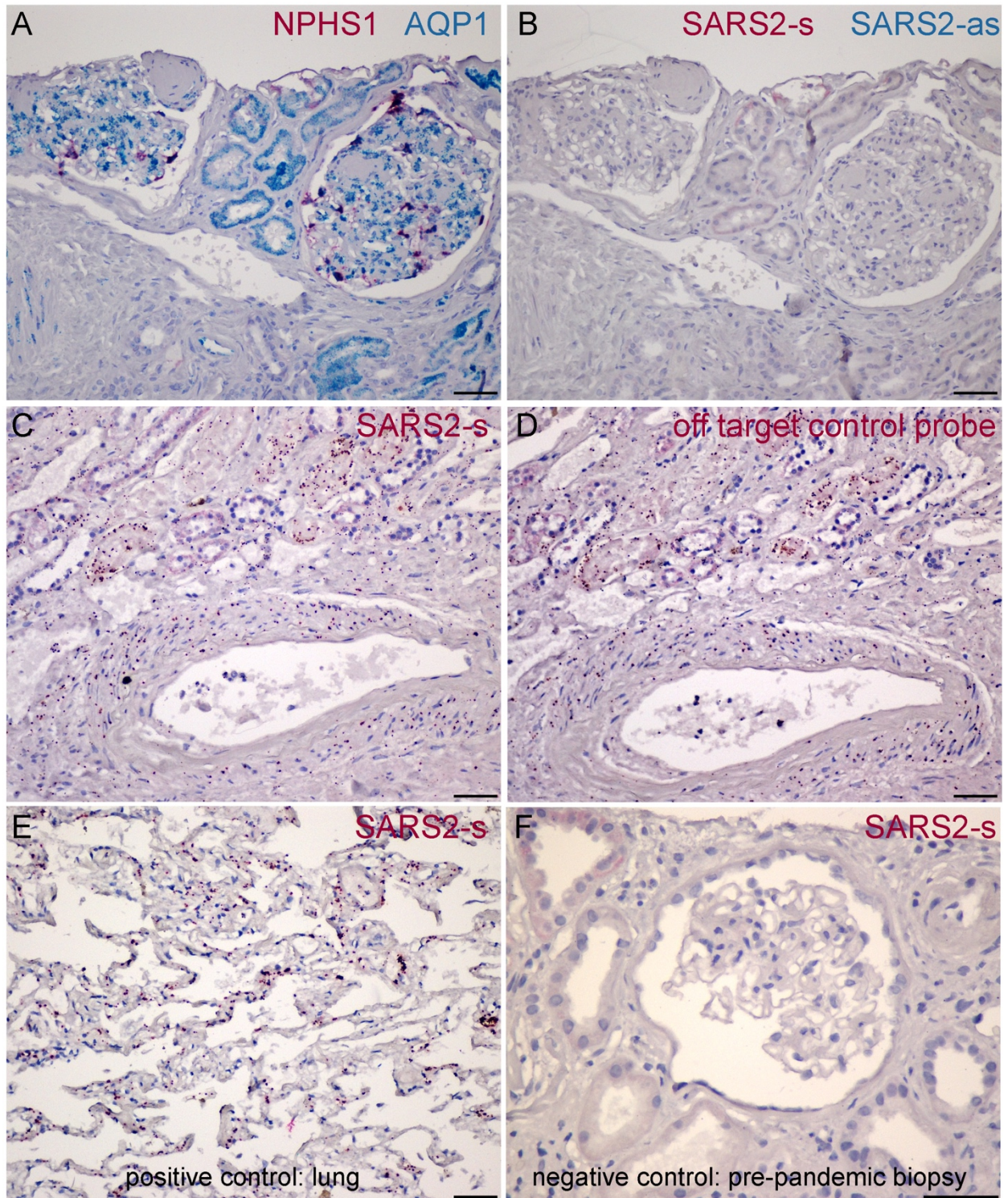
Reagent list

Methods	Reagent	Company	Catalog number	application details
RNA in situ hybridization	RNAscope 2.5 HD Duplex kit (manual)	ACDBio	322430	
	RNAscope 2.5 HD RED Assay (manual)	ACDBio	322350	
	<i>Hs-APOL1-No-XMm</i>	ACDBio	459791	channel 1 or channel 2 if in duplex assay
	<i>Hs-AQP1</i>	ACDBio	421831	channel 1 or channel 2 if in duplex assay
	<i>Hs-NPHS1</i>	ACDBio	416071	channel 1 or channel 2 if in duplex assay
	<i>Hs-ACE2</i>	ACDBio	848151	channel 1 or channel 2 if in duplex assay
	<i>V-nCoV2019-S</i>	ACDBio	848561	channel 1 or channel 2 if in duplex assay
	<i>V-nCoV2019-S-sense</i>	ACDBio	845701	channel 1 or channel 2 if in duplex assay
	<i>V-nCoV2019-orf1ab-sense</i>	ACDBio	859151	channel 1 or channel 2 if in duplex assay
	EcoMount	ACDBio	EM897L	
Fluorescent in situ hybridization	bacterial taxa universal 16s	Invitrogen	EUB388	GCTGCCTCCCGTAGGAGT
Immunofluorescence microscopy	anti-human APOL1 rabbit polyclonal	Sigma	HPA018885	1:400 dilution (note: this lot is no longer available for purchase from manufacturer)
	anti-human CD3 rabbit monoclonal	Abcam	ab16669	1:3000 dilution
	anti-human CD68 mouse monoclonal	Abcam	ab955	1:400 dilution
	anti-human ACE2 rabbit monoclonal	Invitrogen	MA5-32307	1:100 dilution
	anti-SARS-CoV-2 nucleocapsid (spike) mouse monoclonal	Invitrogen	MA1-7404	1:200 dilution
	Goat anti-rabbit Cy3	Jackson Labs.	111-165-144	5 µg/ml
	Goat anti-mouse Cy3	Jackson Labs.	115-165-146	5 µg/ml
	Goat anti-rabbit Alexafluor 488	Invitrogen	A11034	5 µg/ml
	Goat anti-mouse Alexafluor 488	Invitrogen	A11029	5 µg/ml
	Slowfade Diamond mountant with DAPI	Invitrogen	S36964	

Supplemental Table 1: Details on subjects in biopsy cohort.

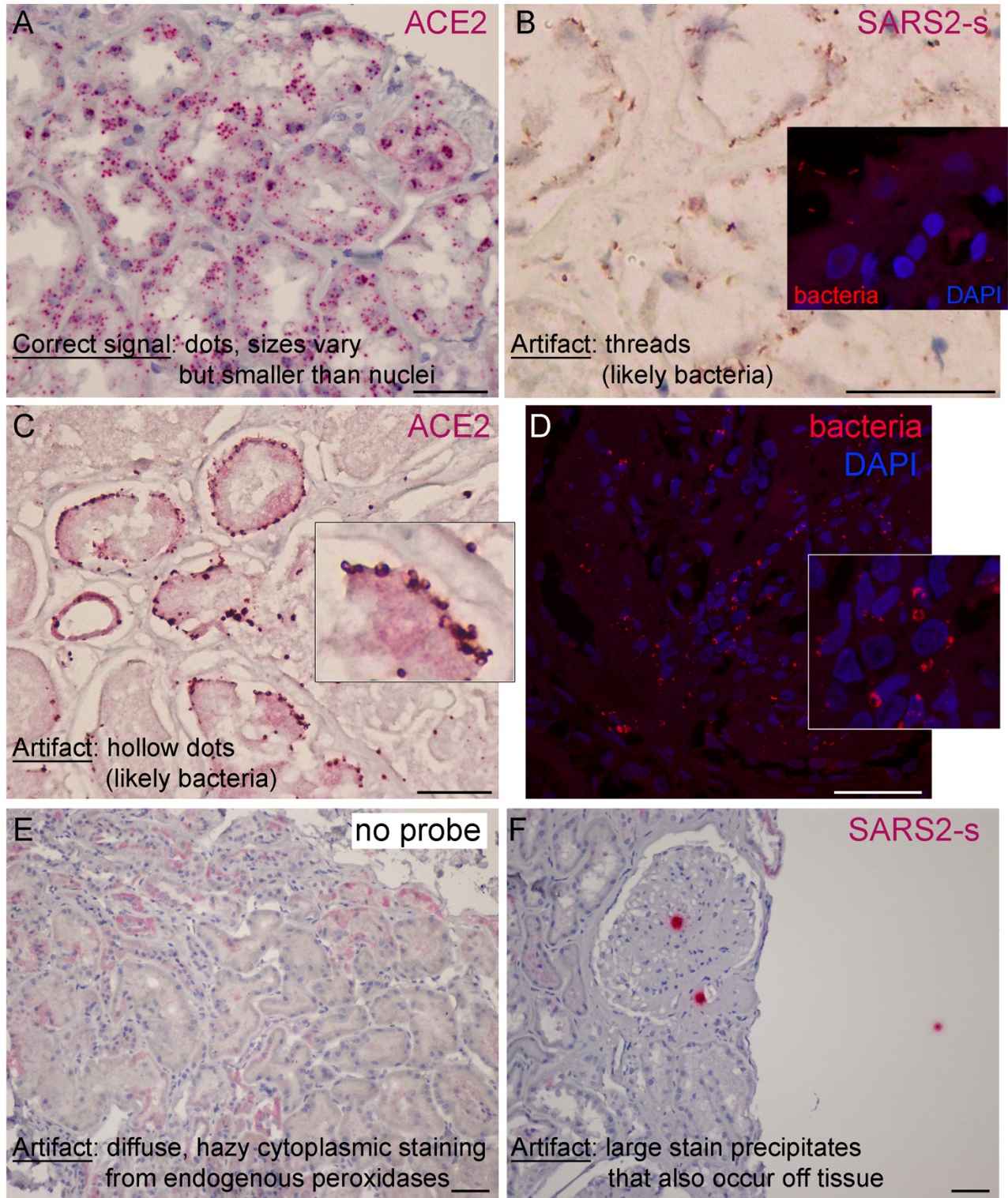
sex	age	APOL1 genotype	biopsy diagnosis	clinical AKI	prior CKD diagnosis	other clinical data	pre-existing diabetes	pre-existing hypertension	
F	46	G1G1	Collapsing FSGS		yes				
M	71	G2G2	Collapsing FSGS	yes	yes		yes	yes	
F	47	G1G1	Collapsing FSGS	yes	yes			yes	
F	64	G1G1	Collapsing FSGS	yes			yes	yes	
M	54	G1G2	Collapsing FSGS	yes	yes			yes	
M	66	G1G2	Collapsing FSGS	yes	yes			yes	
M	77	G0G1	Collapsing FSGS	yes				yes	
M	45	G0G1	Collapsing FSGS	yes				yes	
F	55	G0G1	Collapsing FSGS	yes				yes	
M	46	G2G2	Collapsing FSGS	yes					
F	77	G1G1	Collapsing FSGS	yes				yes	
M	39	G0G0	Collapsing FSGS	yes	yes				
M	45	G0G1	Collapsing FSGS						
F	67	G0G1*	Collapsing FSGS	yes	yes	transplant recipient			
F	56	G1G2	FSGS nos	yes			yes	yes	
F	30	G1G1	FSGS nos				yes	yes	
F	61	G1G1	FSGS nos					yes	
M	44	G0G2	Podocytopathy		yes				
F	44	G0G0	Podocytopathy				yes		
F	51	G0G0	Podocytopathy				yes		
F	51	G1G2	Podocytopathy	yes			yes	yes	
F	69	G0G0	Podocytopathy				yes	yes	
F	60	G1G1	Podocytopathy			pre-existing lupus	yes	yes	
M	21	G0G0	Podocytopathy	yes					
F	67	G0G2*	acute rejection	yes	yes	transplant recipient	yes	yes	
M	45	G0G0*	acute rejection	yes	yes	transplant recipient			
COVID negative controls									
M	59	G0G0	FSGS nos		yes		yes	yes	
M	53	G0G0	FSGS nos		yes			yes	
M	53	G0G0	FSGS nos		yes			yes	
M	32	G0G0	IgA nephropathy		yes				
F	65	G0G0*	normal renal parenchyma (implant biopsy)						

* graft/donor genotype



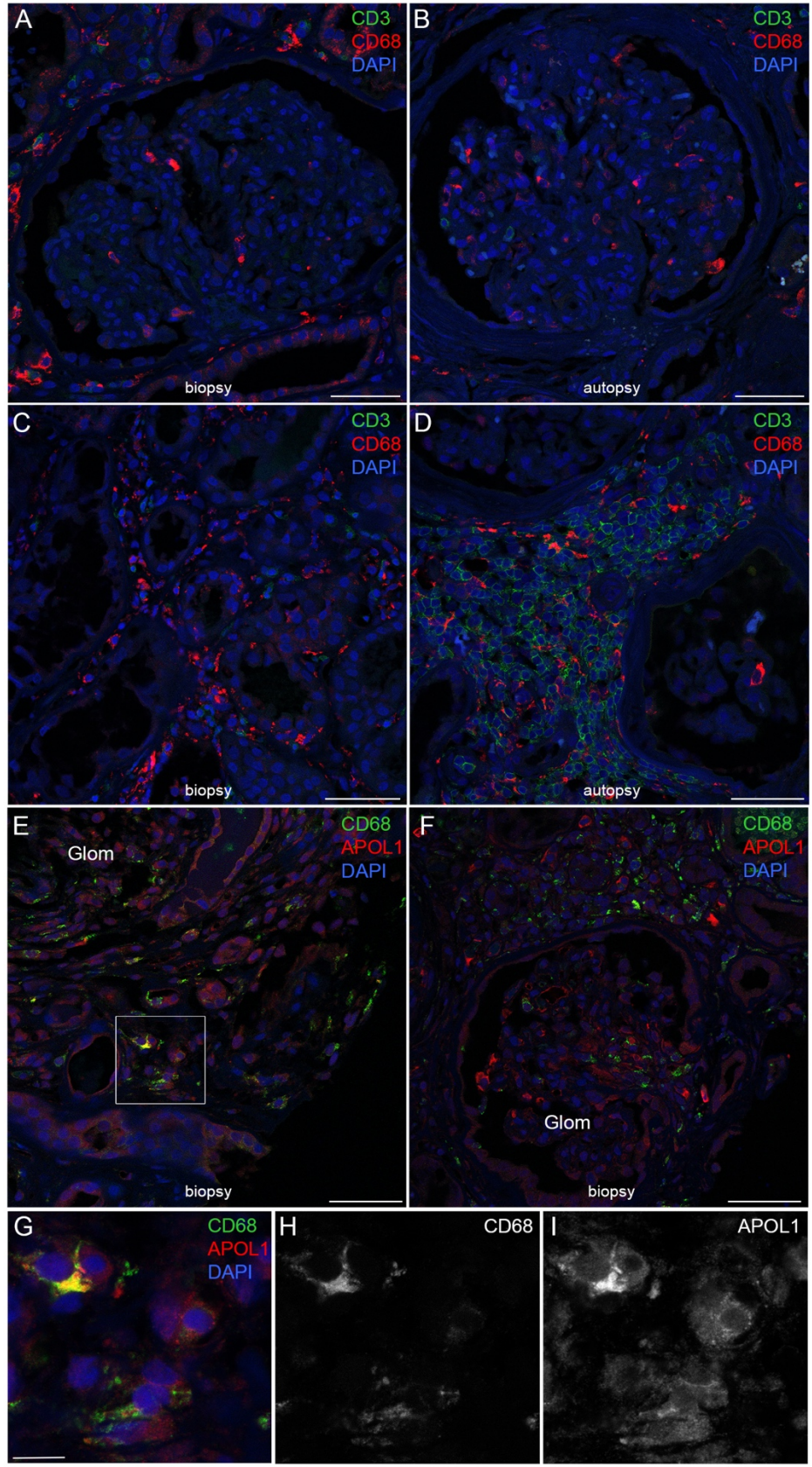
Supplemental Figure 1. Assay and tissue validation with control probes and control tissues.

Supplemental Figure 1. Representative results using ACDBio RNAscope in situ hybridization manual assay using either one probe (singleplex, fast red chromogen) or two probes (duplex, fast red and fast green chromogens). Slides are counterstained with hematoxylin. **A.** Example of tissue quality control using the RNAscope duplex assay with positive control probes for the genes for nephrin (*NPHS1*, expected signal in podocytes) and aquaporin 1 (*AQP1*, expected signal in proximal tubules and glomerular endothelia). Tissues that failed these two probes were considered to not pass quality control and indicated the tissue handling and storage conditions were not adequate to preserve RNA. This quality control step eliminated potential false negatives. **B.** Serial section to panel A showing absence of SARS-CoV-2 (SARS2) RNA using both a probe to detect viral genomic RNA (sense, s) or viral RNAs generated during active replication (antisense, as). **C, D.** Example of a suspect artifactual positive signal (**C**) verified by comparing with an off target probe (**D**) in serial sections. Probe in panel D should be negative but generated a similar pattern to panel C which was likely bacterial contamination (see supplemental Figure 2). **E.** Lung tissue obtained from COVID autopsy case used as a positive control. **F.** Biopsies from SARS-CoV-2 negative subjects (n=5), including biopsies obtained prior to the pandemic, were used as negative controls. Scale bar = 50µm.



Supplemental Figure 2. Common artifacts (false positives) of the ACDBio RNAscope in situ hybridization method using chromogenic stains.

Supplemental Figure 2. ACDBio RNAscope in situ hybridization manual assay using one probe (fast red chromogen), counterstained with hematoxylin. **A.** The correct signal from the RNAscope assay is a dot of varying sizes, but dots are smaller than nuclei. They represent single molecule detection and can be quantified using standard image analysis techniques. **B-D.** Bacterial contamination, which was most problematic in the autopsy specimens, generated positive signals that frequently were not dots, but either threads (panel **B**) or hollow dots or curved structures (panel **C**). Specimens that exhibited this pattern were re-examined with an off-target probe (see sFig 1 C, D) or bacterial contamination was confirmed by using a fluorescent in situ hybridization procedures with a universal (pan-bacteria) 16s rRNA probe (panel **D** and panel **C** inset); DAPI as a nuclear stain. **E.** Another common artifact is the bleed-through or inadequate blocking of endogenous peroxidases, resulting in a diffuse or hazy cytoplasmic staining most commonly observed in tubules. This artifact was confirmed/ruled-out by processing additional sections through the complete in situ procedure but excluding the probe and replacing it with probe diluent (no probe control). **F.** Another artifact is the non-specific deposition of stain precipitates, which can be discerned from a *bona fide* RNA detection signal as the precipitates typically form dots larger than the size of nuclei and are also observed off the tissue section. This artifact was confirmed/ruled-out by repeating the assay on additional sections to determine if the signal was reproducible. Scale bar = 50 μ m.



Supplemental Figure 3. Immune cells in autopsy and biopsy kidney tissue.

Supplemental Figure 3. Immune cells in autopsy and biopsy kidney tissue.

Immunofluorescence for CD3 (pan T cell marker) and CD68 (monocyte/macrophage marker), with DAPI as nuclear stain. **A, C.** Biopsies had varied degrees of immune cell infiltrates, but those with immune cell infiltrates were primarily populated by CD68 positive cells with few CD3 positive cells in both glomeruli (A) and tubulointerstitium (C). **B, D.** Autopsy specimens also had varying degrees of immune cell infiltrates, but those with infiltrates were populated by both CD3 and CD68 positive cells in both glomeruli (B) and tubulointerstitium (D). **E-I.** In biopsies, CD68 positive immune cells expressed apolipoprotein L1 (APOL1). **E, F.** CD68-positive immune cells in glomeruli (Glom) and interstitium also express APOL1. It has been shown previously that cells of immune lineages including macrophages, NK cells and T cells express *APOL1* and may participate in events that effect outcomes associated with kidney transplantation.⁵⁻⁸ **G.** Boxed region in panel E at higher magnification with individual fluorescent channels for CD68 and APOL1 shown in panels **H** and **I** respectively as monochromatic images. Panels A-F, scale bar = 50 μ m. Panels G-I, scale bar = 10 μ m.

Supplemental References

1. Madhavan SM, O'Toole JF, Konieczkowski M, Ganesan S, Bruggeman LA, Sedor JR: APOL1 localization in normal kidney and nondiabetic kidney disease. *J Am Soc Nephrol*, 22: 2119-2128, 2011 10.1681/asn.2011010069
2. Blessing NA, Wu Z, Madhavan SM, Choy JW, Chen M, Shin MK, et al.: Lack of APOL1 in proximal tubules of normal human kidneys and proteinuric APOL1 transgenic mouse kidneys. *PLoS One*, 16: e0253197, 2021 10.1371/journal.pone.0253197
3. Daims H, Brühl A, Amann R, Schleifer KH, Wagner M: The domain-specific probe EUB338 is insufficient for the detection of all Bacteria: development and evaluation of a more comprehensive probe set. *Syst Appl Microbiol*, 22: 434-444, 1999 10.1016/s0723-2020(99)80053-8
4. Bankhead P, Loughrey MB, Fernández JA, Dombrowski Y, McArt DG, Dunne PD, et al.: QuPath: Open source software for digital pathology image analysis. *Scientific Reports*, 7: 16878, 2017 10.1038/s41598-017-17204-5
5. Zhang Z, Sun Z, Fu J, Lin Q, Banu K, Chauhan K, et al.: Recipient APOL1 risk alleles associate with death-censored renal allograft survival and rejection episodes. *J Clin Invest*, 131, 2021 10.1172/jci146643
6. Taylor HE, Khatua AK, Popik W: The innate immune factor apolipoprotein L1 restricts HIV-1 infection. *J Virol*, 88: 592-603, 2014 10.1128/jvi.02828-13
7. Lee H, Fessler MB, Qu P, Heymann J, Kopp JB: Macrophage polarization in innate immune responses contributing to pathogenesis of chronic kidney disease. *BMC Nephrol*, 21: 270, 2020 10.1186/s12882-020-01921-7
8. Ryu JH, Ge M, Merscher S, Rosenberg AZ, Desante M, Roshanravan H, et al.: APOL1 renal risk variants promote cholesterol accumulation in tissues and cultured macrophages from APOL1 transgenic mice. *PLoS One*, 14: e0211559, 2019 10.1371/journal.pone.0211559